Xu et al. Nanoscale Research Letters (2017) 12:311
DOI 10.1186/s11671-017-2068-y

Nanoscale Research Letters

NANO EXPRESS Open Access

# In Situ Analysis of Oxygen Vacancies and Band Alignment in $HfO_2$/TiN Structure for CMOS Applications

Da-Peng Xu, Lin-Jie Yu, Xu-Dong Chen, Lin Chen*, Qing-Qing Sun*, Hao Zhu, Hong-Liang Lu, Peng Zhou, Shi-Jin Ding and David Wei Zhang

## Abstract

The density of oxygen vacancies characterization in high-k/metal gate is significant for semiconductor device fabrication. In this work, a new approach was demonstrated to detect the density of oxygen vacancies by in situ x-ray photoelectron spectroscopy (XPS) and ultraviolet photoelectron spectroscopy (UPS) measurement. Moreover, the band alignment of the structure with optical band gap measured by spectroscopic ellipsometry (SE) and valence band offset by UPS were reported. The specific areal density of oxygen vacancies in high-k dielectric of $HfO_2$/TiN was obtained by fitting the experiment data to be $8.202 \times 10^{10} cm^{-2}$. This study would provide an effective approach to characterize the oxygen vacancies based defects which cause threshold voltage shifts and enormous gate leakage in modern MOSFET devices.

**Keywords:** Oxygen vacancies, Band alignment, In situ XPS, UPS, Ellipsometry

## Background

With the conventional Si-based CMOS technology scaling down, high-k/metal gate are regarded as one of the most important structures in modern MOS devices. Among various types of High-k/metal gate, $HfO_2$/TiN structure has been proved to be one of the standards in high-k integration in CMOS technology below 28 nm technical node due to its large band offsets, thermodynamic stability in contact with Si, and excellent high-frequency response [1–6]. However, the oxygen vacancies in $HfO_2$ is the main obstacle for practical application: The oxygen vacancies in high-k dielectric would cause Threshold Voltage Shifts (TVS) [7] and enormous Gate leakage [8] which may affect MOSFET performance. Moreover, the presence of oxygen vacancies generate a high concentration of charge traps and scattering centers [9], which caused the degradation of mobility in the channel of MOSFET. Few works studied the determination of the density of oxygen vacancies in the $HfO_2$ film through experimental methods. In this work, we use *In-situ* [10] Measurement System to investigate the feature of $HfO_2$/TiN Structure manufactured by PVD and ALD, with X-ray Photoelectron Spectroscopy (XPS) and Ultraviolet Photoelectron Spectroscopy (UPS) applied to get the composition of the film and the work functions of TiN metal with different thickness of $HfO_2$ dielectric in 0.2, 0.5, 0.8, 1.2, 1.6, 2.0, 2.5 and 3.0 nm. By fitting the curves of different TiN work functions due to the ultraviolet activation by UPS and extracting the fitted parameters, the density of oxygen vacancies in $HfO_2$ film can be achieved. Moreover, both the band alignment of the structure with optical band gap measured by spectroscopic ellipsometry (SE) and valence band offset by UPS are also reported in this work.

## Methods

The structure of Fig. 1 (a) has been manufactured by SPECS *In-Situ* Cluster System and Picosun ALD system. Firstly, 24 nm TiN was deposited on highly-doped silicon wafer by SPECS PVD Sputtering for 3000 s with Titanium target and Nitrogen. Highly-doped silicon wafer was used to eliminate the accumulation of the charge effect during UPS measurement caused by negative substrate voltage. Then the original work function of TiN was measured by UPS. Subsequently, 0.2, 0.5, 0.8,

* Correspondence: linchen@fudan.edu.cn; qqsun@fudan.edu.cn
State Key Laboratory of ASIC and System, School of Microelectronics, Fudan University, Shanghai 200433, China

Springer Open

© The Author(s). 2017 **Open Access** This article is distributed under the terms of the Creative Commons Attribution 4.0 International License (http://creativecommons.org/licenses/by/4.0/), which permits unrestricted use, distribution, and reproduction in any medium, provided you give appropriate credit to the original author(s) and the source, provide a link to the Creative Commons license, and indicate if changes were made.

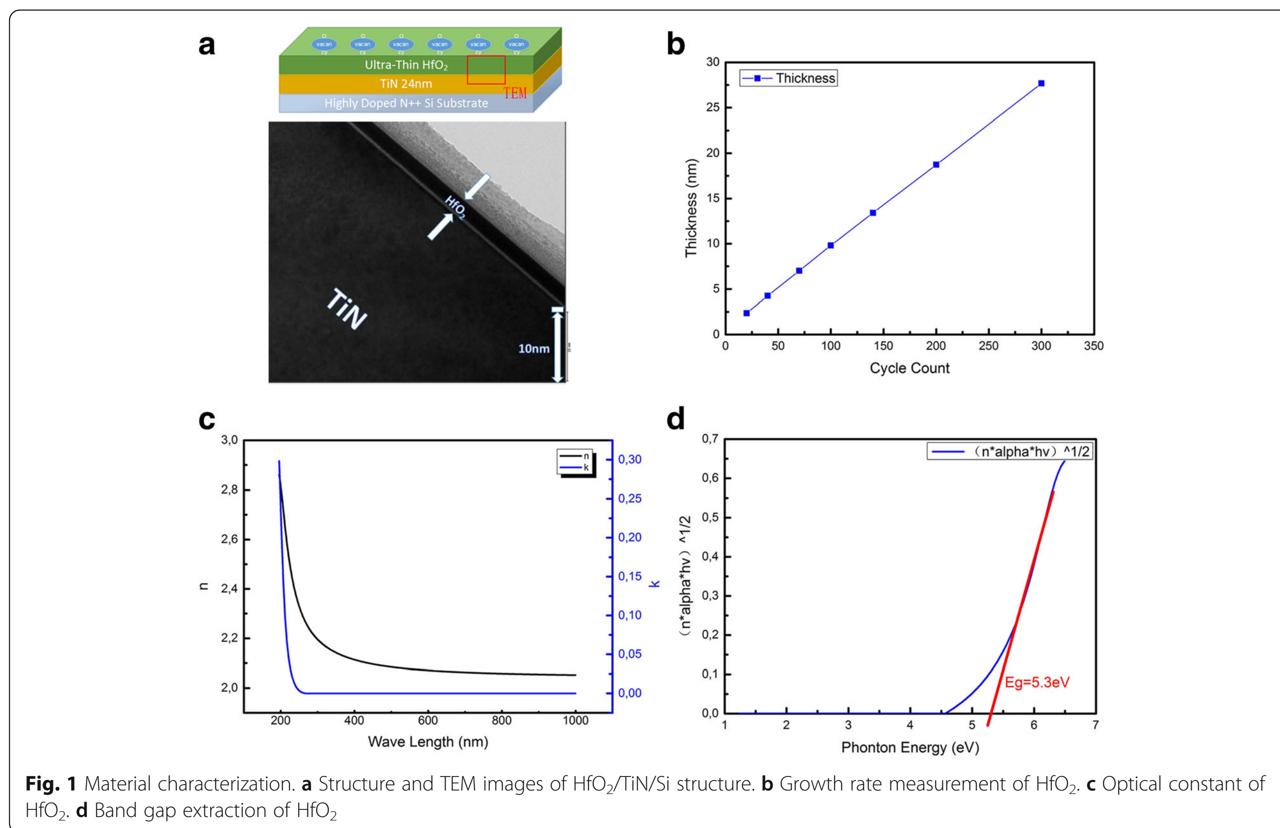


**Fig. 1** Material characterization. **a** Structure and TEM images of $HfO_2$/TiN/Si structure. **b** Growth rate measurement of $HfO_2$. **c** Optical constant of $HfO_2$. **d** Band gap extraction of $HfO_2$

1.2, 1.6, 2.0, 2.5 and 3.0 nm $HfO_2$ were deposited on the TiN surface by Picosun ALD with TEMAH precursor (70 °C) and $H_2O$ at certain reactor temperature (250 °C) [11] in high vacuum chamber. During each thickness of $HfO_2$ growing process (0.2, 0.5, 0.8, 1.2, 1.6, 2.0, 2.5 and 3.0 nm), the sample was transferred to the XPS chamber. Then, *in-situ* XPS and UPS were measured with mono-Al target X-ray source and HeI Ultraviolet source utilized in XPS and UPS. Also, we apply -5 V voltage to the substrate holder during UPS measurement for shifting our spectrum position to observe the cutoff edge, respectfully. The manufacture and measurement process were *In-situ* process in high vacuum chambers. The composition of the film, the work function of the TiN and the Valence Band Offset (VBO) of TiN/$HfO_2$ were also calculated from the results. The growth rate of ALD-$HfO_2$ was measured by J.A.Woollam *In-situ* SE with different thickness of $HfO_2$ deposited instantly on Si substrate by Picosun ALD. The optical band gap of $HfO_2$ can also be extracted from this measurement. With TiN work function, $HfO_2$/TiN VBO and optical band gap of $HfO_2$ ($E_g$), the band alignment of $HfO_2$/TiN has been studied in this paper. Moreover, oxygen vacancies can be calculated from the change of the TiN work function caused by the ultraviolet stimulus of oxygen vacancies in $HfO_2$ layer by UPS during the growth of $HfO_2$.

## Results and Discussion

The structure and TEM images of $HfO_2$/TiN/Si has been shown in Fig. 1(a). The structure of our test chip is a sandwich structure with $HfO_2$, TiN and silicon substrate. The thickness of $HfO_2$ and TiN is 3 nm and 24 nm after the whole process. The ALD growth rate, the optical constant and the band gap of $HfO_2$ has been presented in Fig. 1(b), (c) and (d) which were measured by *In-situ* SE. From Fig. 1(b), 20, 40, 70, 100, 140, 200, 300 cycles $HfO_2$ were deposited directly on the clean 4-inch silicon wafer substrate by ALD process to measure the growth rate of $HfO_2$. The thickness of 20, 40, 70, 100, 140, 200, 300 cycles $HfO_2$ were measured to be 2.36, 4.25, 7.01, 9.80, 13.42, 18.73 and 27.67 nm. From the slope of the line, the growth rate of $HfO_2$ for the experiment is 0.09 nm/cycle which is reasonable in ALD deposition [11]. Moreover, the optical constant of the film is presented in Fig. 1(c). From the Figure, the index of refraction (n) of the $HfO_2$ film decrease with the increasing of λ. The index of refraction (n) of the $HfO_2$ film at 632 nm is 2.07 which is slightly larger than the standard 1.9 due to the defect of the film but in good agreement with Liu et al. [12]. The k value of the $HfO_2$ is not zero in low λ which indicates the absorption of the film, which can simultaneously indicate the defects in $HfO_2$. The optical bandgap of the $HfO_2$ was 5.3 eV in

our work determined by plotting the empirical expression $(n\alpha h\gamma)^{\frac{1}{2}}$ versus hγ, as shown in Fig. 1(d), where n, α and hγ is the index of refraction, the absorption coefficient and the photon energy as described in Yang et al. [13]. The extracted $E_g$ value (5.3 eV) is in good agreement with previously reported values from 5.25 eV to 5.8 eV for $HfO_2$ [14–16] in different references.

The XPS diagram of $HfO_2$ (2 nm)/TiN structure was shown in Fig. 2 after calibrated by C 1 s Binding Energy (284.6 eV).The elemental stoichiometry Hf : O was calculated to be 1:1.96 from the XPS data. Because of the limit of the measurement depth of X-ray source, there were only five kinds of element (Ti, N, O, Hf and C), which is presented in Fig. 2 (except the Carbon). Two components were fitted to the O1s spectrum in Fig. 2(a) for 531.4 eV (Ti-O) and 529.6 eV (Hf-O) and there were two peaks of Hf 4d diagram because of the energy level splitting of 4d3 and 4d5 in Fig. 2(b). In Fig. 2(c), Ti was not accurate enough to fit for the fact that the TiN film actually is the mixture of $Ti_2N_2$, $Ti_3N_4$, TiON interface and some other their compounds which also was covered by a layer of $HfO_2$. Fig. 2(d) is the XPS diagram of N 1 s which can prove the existence of TiN layer. The work function of the TiN was measured to be 4.50 eV in Fig. 3(a) by UPS, which was calculated by the energy of HeI (21.22 eV) ultraviolet, the Fermi Edge (0.02 eV) and the Cut-off Edge (16.74 eV) of UPS diagram. The Valence Band Offset (VBO) was measured to be 3.01 eV by the UPS of 2.0 nm $HfO_2$ deposited on TiN in Fig. 3(b). With TiN work function (4.5 eV), $HfO_2$/TiN VBO (3.0 eV) and optical band gap of $HfO_2$ (5.3 eV), the band alignment of $HfO_2$/TiN has been reported in Fig. 4. The Conduction Band Offset (CBO) is 2.3 eV as presented in Fig. 4(a).The results are reasonable compared to calculation result 3.0 eV [17] using WM method based on ab initio calculations.

The UPS spectrum of 0.2, 0.5, 0.8, 1.2, 1.6, 2.0, 2.5 and 3.0 nm of $HfO_2$ deposited on the TiN has been given in Fig. 5(a). The Fermi Edge of the UPS is measured by the point of inflection of the curve and the Cut-off Edge of the UPS is chosen by the middle point of the maximum and the minimum. The Fermi Edge is around zero point due to the charge effect, and the Cut-off Edge is shifted to the direction of high binding energy which indicates the decrease of the TiN work function with increasing $HfO_2$ thickness from Fig. 5(a). The difference of the work function was caused by the oxygen vacancies activation with HeI UV source applied during the UPS measurement. The work function of the 2.5 nm and 3 nm $HfO_2$ is not correct due to the charge effect caused by the limited depth of UPS. The gap between 2.0 and 2.5 nm in Fig. 5(b) and the nearly same curve of the UPS spectrum in Fig. 5(a) indicates that those two points should beyond the range of UPS depth.

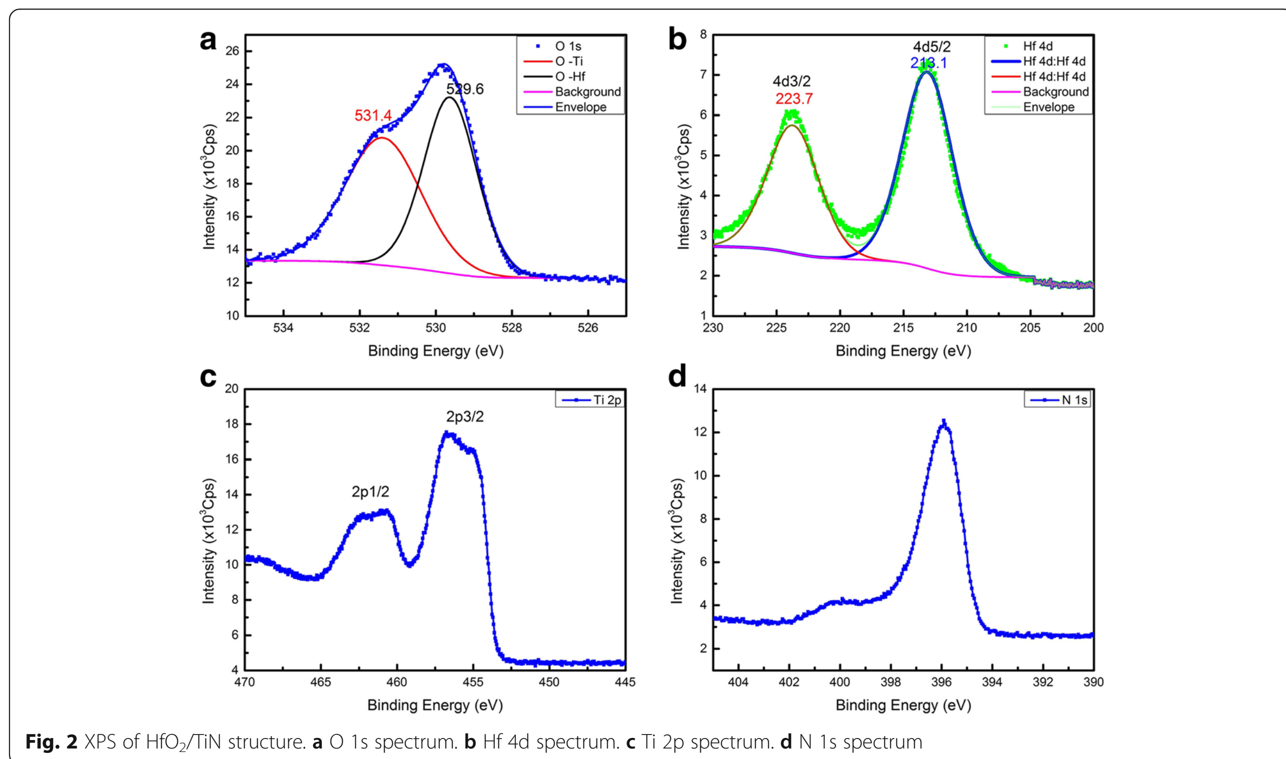


**Fig. 2** XPS of $HfO_2$/TiN structure. **a** O 1s spectrum. **b** Hf 4d spectrum. **c** Ti 2p spectrum. **d** N 1s spectrum

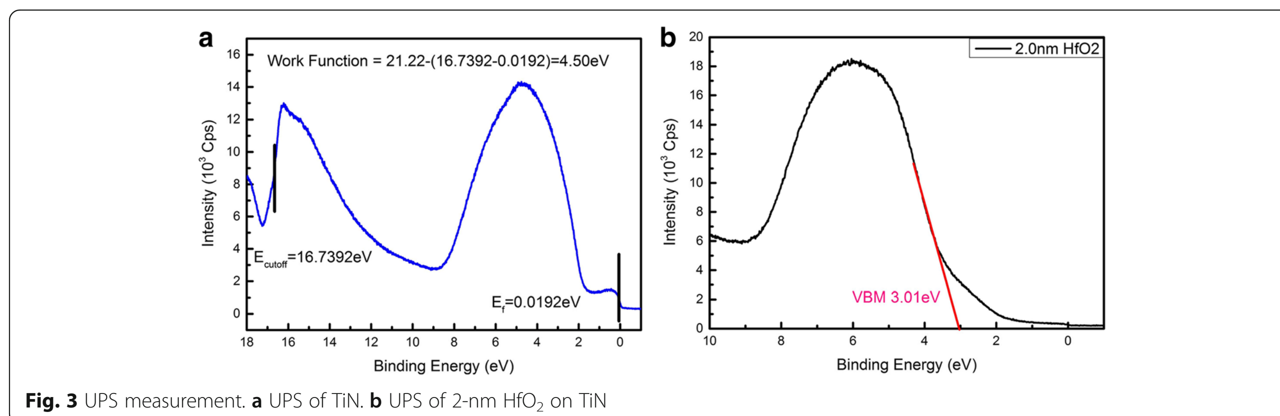


**Fig. 3** UPS measurement. **a** UPS of TiN. **b** UPS of 2-nm $HfO_2$ on TiN

The density of oxygen vacancies was extracted from the experiment data with the simple capacitor physics equation. Fig. 4(b) is the TiN/$HfO_2$ structure from left to right. In Fig. 4(b), take x to x + dx as a parallel capacitor. According to the basic charge equation,

$$\mathrm{Q} = \mathrm{C} \times \mathrm{V} \tag{1}$$

Where Q is the charge, C is the capacitor and V is the voltage between the capacitor.

Considering the activated interface trap in $HfO_2$/TiN interface and the oxygen vacancies density in body, we got

$$\mathrm{Q}_{it} + \delta_x x S = \frac{\varepsilon_{HfO2} S}{dx} dV \tag{2}$$

Where $\mathrm{Q}_{it}$ is the charge of $HfO_2$/TiN interface trap, $\delta_x$ is the bulk charge density of the oxygen vacancies, $S$ is the area of the wafer and $\varepsilon_{HfO2}$ is the dielectric constant (the relative dielectric constant is 16, which is calculated by SE data and verified by C-V measurement, and the $\varepsilon_0$ is $8.85 \times 10^{-12}$ F/m).

After integration, then note $\mathrm{q}_{it} \equiv \frac{Q_{it}}{S}$, which is the Areal density of the charge of interface trap. The change of the work function in UPS diagram in Fig. 5(b) is caused by the charge of oxygen vacancies. Therefore,

$$\mathrm{V(x)} = \frac{\mathrm{W}_F(\mathrm{x})}{e} = \frac{\delta_x}{2\varepsilon_{HfO2}} x^2 + \frac{q_{it}}{\varepsilon_{HfO2}} x + A \tag{3}$$

Where e is the charge of the electron for $1.6 \times 10^{-19}$C.

After the TiN work function fitting process in Fig. 5(b) by quadratic function, we got $\frac{\delta_x \times e}{2\varepsilon_{HfO2}} = 3.089 \times 10^{14}$ $\left(V \cdot \frac{C}{m^2}\right)$ and $\frac{q_{it} \times e}{\varepsilon_{HfO2}} = 4.077 \times 10^8$ $\left(V \cdot \frac{C}{m}\right)$. After the calculation, the bulk charge density of the oxygen vacancies is

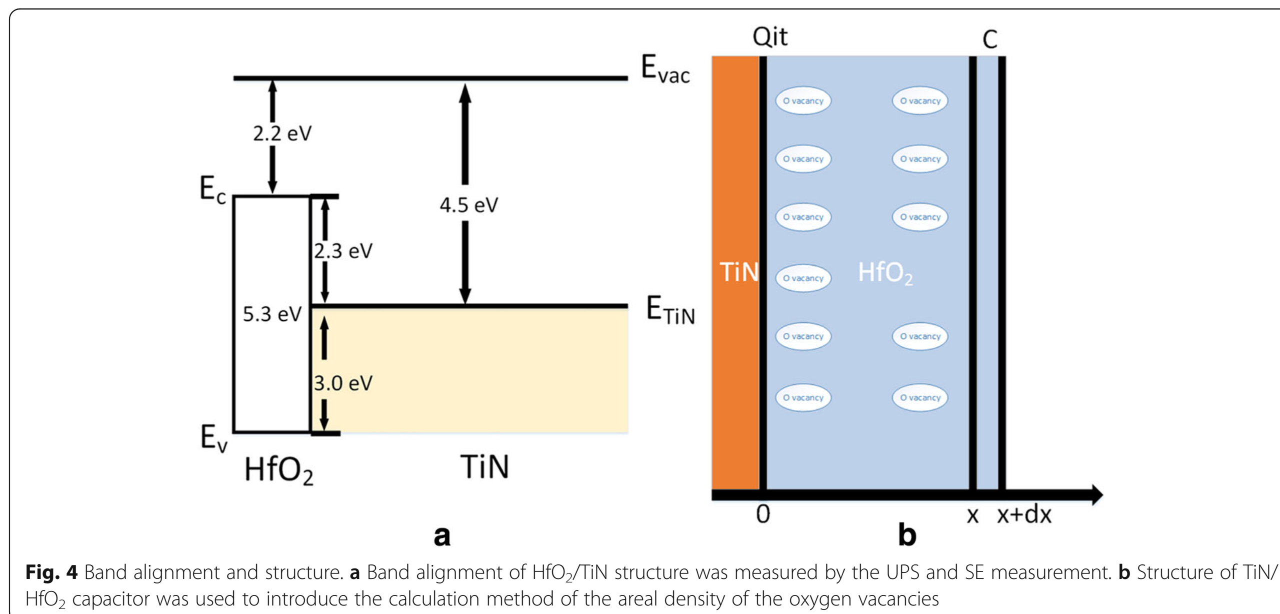


**Fig. 4** Band alignment and structure. **a** Band alignment of $HfO_2$/TiN structure was measured by the UPS and SE measurement. **b** Structure of TiN/$HfO_2$ capacitor was used to introduce the calculation method of the areal density of the oxygen vacancies

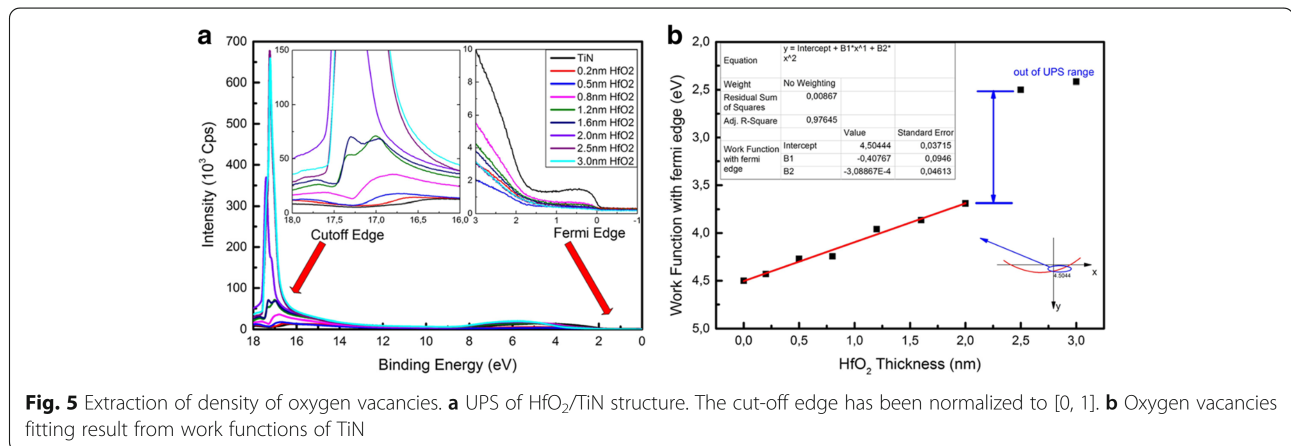


**Fig. 5** Extraction of density of oxygen vacancies. **a** UPS of $HfO_2$/TiN structure. The cut-off edge has been normalized to [0, 1]. **b** Oxygen vacancies fitting result from work functions of TiN

$\delta_x = 5.468 \times 10^{17}\ cm^{-3}$. The oxygen vacancies in $HfO_2$ may exist in five charge states, +2, +1, 0, −1, −2 corresponding to up to four extra electrons in the vicinity of the vacant $O^{2-}$ site [9]. However, the Ultraviolet source from UPS measurement will activate the electron in defects and make the oxygen vacancies to be +2 states. After changed to areal density by multiply the $HfO_2$ thickness (2 nm) and divided by 2 (one oxygen vacancy has two charges), the areal density of the oxygen vacancies is $8.202 \times 10^{10}\ cm^{-2}$ and the areal density of the interface trap is $q_{it} = 3.608 \times 10^{13}\ cm^{-2}$.This result is acceptable because the sample was not annealed in forming gas which would make $q_{it}$ larger.

## Conclusions

In summary, we successfully realized the measurement of the band alignment and the determination of the density of oxygen vacancies by *in-situ* SE, XPS and UPS with different thickness of $HfO_2$ dielectric in 0.2, 0.5, 0.8, 1.2, 1.6, 2.0, 2.5 and 3.0 nm on TiN metal layer. The density of oxygen vacancies was extracted from the experiment data with the simple capacitor physics equation. In TiN/$HfO_2$ Band Alignment, the work function of the $HfO_2$ optical band gap is 5.3 eV,and the VBO and CBO of $HfO_2$/TiN is 3.0 eV and 2.3 eV. The areal density of the oxygen vacancies is calculated to be $8.202 \times 10^{10}\ cm^{-2}$. This method provides a direct way to capture the density of oxygen vacancies of the high-k/metal-gate for advanced semiconductor MOSFETs.

### Abbreviations

SE: Spectroscopic ellipsometry; TVS: Threshold voltage shifts; UPS: Ultraviolet photoelectron spectroscopy; VBO: Valence band offset; XPS: X-ray photoelectron spectroscopy

### Funding

This work was supported by the NSFC (61376092, 51172046, and 61427901), program of Shanghai Subject Chief Scientist (14XD1400900), and the S&T Committee of Shanghai (15DZ1100702, 15DZ1100503), and the "Chen Guang" project was supported by Shanghai Municipal Education Commission and Shanghai Education Development Foundation.

### Authors' Contributions

DPX and XDC made the physical tests, analyzed the results, and drafted the manuscript. LJY carried out the manufacture of the samples. XDC made the optical tests and supplied valuable discussion about the analysis. LC and QQS conceived of the study and participated in its design and coordination. HLL, PZ, SJD, and DWZ participated in the design of the study and helped to draft the manuscript. All authors read and approved the final manuscript.

### Competing Interests

The authors declare that they have no competing interests.

## Publisher's Note

Springer Nature remains neutral with regard to jurisdictional claims in published maps and institutional affiliations.

Received: 27 December 2016 Accepted: 10 April 2017
Published online: 27 April 2017

### References

1. Gusev E, Buchanan D, Cartier E, Kumar A, DiMaria D, Guha S, Callegari A, Zafar S, Jamison PNeumayer D: Ultrathin high-K gate stacks for advanced CMOS devices. *IEEE International Electron Devices Meeting* 2001, 20.21.21-20.21.24.
2. Robertson J (2005) Interfaces and defects of high-K oxides on silicon. Solid State Electron 49:283–293
3. Robertson J, Xiong K, Tse KY: Importance of Oxygen Vacancies in High K Gate Dielectrics. *IEEE International Conference on Integrated Circuit Design and Technology* 2007, 1-4.
4. Robertson J (2000) Band offsets of wide-band-gap oxides and implications for future electronic devices. J Vac Sci Technol B 18:1785–1791
5. Peacock P, Robertson J (2002) Band offsets and Schottky barrier heights of high dielectric constant oxides. J Appl Phys 92:4712–4721
6. Chau R, Doczy M, Doyle B, Datta S, Dewey G, Kavalieros J, Jin B, Metz M, Majumdar ARadosavljevic M: Advanced CMOS transistors in the nanotechnology era for high-performance, low-power logic applications. *7th International Conference on Solid-State and Integrated Circuits Technology* 2004, 26-30.
7. Shiraishi K, Yamada K, Torii K, Akasaka Y, Nakajima K, Konno M, Chikyow T, Kitajima H, Arikado TNara Y (2006) Oxygen-vacancy-induced threshold voltage shifts in Hf-related high-k gate stacks. Thin Solid Films 508:305–310
8. Mao LF, Wang ZO (2008) First-principles simulations of the leakage current in metal–oxide–semiconductor structures caused by oxygen vacancies in $HfO_2$ high-K gate dielectric. Phys Status Solidi A 205:199–203
9. Ramo DM, Shluger A, Gavartin JBersuker G (2007) Theoretical prediction of intrinsic self-trapping of electrons and holes in monoclinic $HfO_2$. Phys Rev Lett 99:155504
10. Kaichev VV, Gladky AY, Prosvirin I, Saraev A, Hävecker M, Knop-Gericke A, Schlögl RBukhtiyarov VI (2013) In situ XPS study of self-sustained oscillations in catalytic oxidation of propane over nickel. Surf Sci 609:113–118

11. Kukli K, Ritala M, Sajavaara T, Keinonen JLeskelä M (2002) Atomic layer deposition of hafnium dioxide films from hafnium tetrakis (ethylmethylamide) and water. Chem Vap Depos 8:199–204
12. Liu X, Ramanathan S, Longdergan A, Srivastava A, Lee E, Seidel TE, Barton JT, Pang DGordon RG (2005) ALD of hafnium oxide thin films from tetrakis (ethylmethylamino) hafnium and ozone. J Electrochem Soc 152:G213–G219
13. Yang W, Fronk M, Geng Y, Chen L, Sun QQ, Gordan OD, Zahn DR, Zhang DW (2015) Optical properties and bandgap evolution of ALD HfSiOx films. Nanoscale Res Lett 10:32
14. Nguyen N, Davydov AV, Chandler-Horowitz D, Frank MM (2005) Sub-bandgap defect states in polycrystalline hafnium oxide and their suppression by admixture of silicon. Appl Phys Lett 87:192903
15. Lim SG, Kriventsov S, Jackson TN, Haeni JH, Schlom DG, Balbashov AM, Uecker R, Reiche P, Freeouf JL, Lucovsky G (2002) Dielectric functions and optical bandgaps of high-K dielectrics for metal-oxide-semiconductor field-effect transistors by far ultraviolet spectroscopic ellipsometry. J Appl Phys 91:4500–4505
16. VV A' e, Stesmans A, Tsai W (2003) Determination of interface energy band diagram between (100) Si and mixed Al–Hf oxides using internal electron photoemission. Appl Phys Lett 82:245–247
17. Fonseca LRC, Knizhnik AA (2006) First-principles calculation of the TiN effective work function on $SiO_2$ and on $HfO_2$. Phys Rev B 74:195304

**Submit your manuscript to a SpringerOpen journal and benefit from:**

- ► Convenient online submission
- ► Rigorous peer review
- ► Immediate publication on acceptance
- ► Open access: articles freely available online
- ► High visibility within the field
- ► Retaining the copyright to your article

**Submit your next manuscript at ► springeropen.com**